Probing the Polaronic Landscape in Bi₄TaO₈X Perovskite Oxyhalides Photocatalysts

THE JOURNAL OF PHYSICAL CHEMISTRY C
A JOURNAL OF THE AMERICAN CHEMICAL SOCIETY

pubs.acs.org/JPCC
Article

Probing the Polaronic Landscape in Bi_4TaO_8X Perovskite Oxyhalides Photocatalysts

Hassan Ouhbi and Julia Wiktor*

Cite This: J. Phys. Chem. C 2023, 127, 20965−20970
Read Online

ACCESS | Metrics & More | Article Recommendations

ABSTRACT: Bismuth perovskite oxyhalides Bi_4TaO_8X (X = Cl, Br) are a promising class of photocatalysts due to their resistance to self-decomposition, a property often lacking in other photocatalysts. In order for them to efficiently carry out photocatalytic reactions, it is essential that the diffusion of photogenerated excess charges is not disrupted, such as by the formation of polarons, during transport to the surface, where the reactions take place. We here use a Koopmans-compliant hybrid functional to investigate the behavior of the photogenerated holes and electrons. We first demonstrate that electron polarons are unstable in these materials. Excess holes, on the other hand, localize and alter the atomic structure locally, leading to the formation of various polaronic configurations. Our results show that hole polarons are highly stable at the perovskite block [MO_4] and possess features that are similar to those found for holes in $NaTaO_3$. Furthermore, we find that the presence of two holes results in the occurrence of bipolaronic states, which are accompanied by the formation of O−O dimers. Finally, we show that holes do not localize within the halide block [X], in contrast to oxyhalides BiOX (X = Cl, Br), suggesting that Bi_4TaO_8X are more resistant to self-oxidation of X^-, in accordance with the higher stability reported in experimental studies.

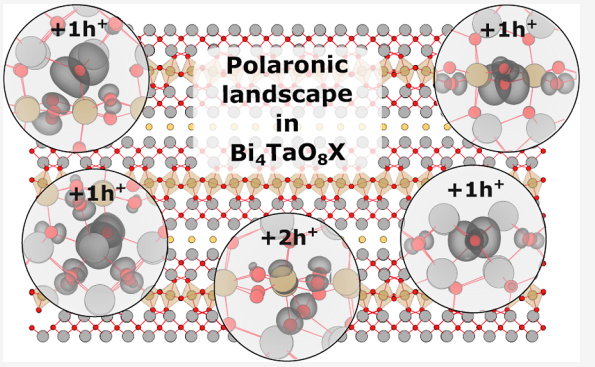

INTRODUCTION

Photocatalytic water splitting using semiconductor catalysts is a promising technique for producing green hydrogen. To achieve high photoactivity, a catalyst should have a band gap below 3 eV, and the valence-band and conduction-band edges of the semiconductor material should be straddling the redox potentials for H^+/H_2 and H_2O/O_2. In addition to these, the photocatalyst should exhibit low electron and hole recombination rates. After years of research, various materials such as perovskite oxynitrides (e.g., $BaTaO_2N$ and $SrTaO_2N$) have been found to exhibit promising photoelectrochemical activity under visible light.[1−3] However, these materials are prone to self-oxidation during the reaction due to the oxidation of N^{3-} by the photogenerated holes. An alternative is the Sillén−Aurivillius perovskite oxyhalides Bi_4TaO_8X (X = Cl, Br), which exhibit high stability and efficiency under visible light.[4−6] These perovskite oxyhalides are characterized by the alternating stacking of Aurivillius perovskite blocks and Sillén blocks[7] (see Figure 1). According to density functional theory (DFT) studies, their valence band maximum (VBM) is mostly composed of O 2p orbitals rather than Xp orbitals, yet its position is much more negative than that of typical oxyhalides (BiOX).[5] Consequently, Bi_4TaO_8X has a narrow band gap (2.50−2.55 eV), which enables them to absorb visible light.[8] The high stability of these materials has been attributed to the dominance of the dispersive O 2p band in the VBM. In other mixed-anion materials, like BiOX oxyhalides, the density of states near VBM is mostly related to the p orbitals of nonoxide anions, which can easily self-oxidize due to hole localization. Meanwhile, oxygen anions are more stable; therefore, the photogenerated holes populating O 2p orbitals do not lead to self-decomposition but rather to water oxidation.[4,9] However, this reaction could be disrupted when photogenerated holes are self-trapped and form polarons. On the other hand, hole trapping could enable electrons to live longer and thus lead to the promotion of reduction reactions such as hydrogen evolution. Therefore, understanding the behavior of the photogenerated charges is of paramount importance to optimize photocatalysts for efficient solar energy conversion.

We recently investigated the behavior of holes and electrons in perovskite tantalates and bismuth oxyhalides.[10,11] We demonstrated that hole polarons are stable and exhibit different localization modes. For instance in BiOBr, we found that holes localize in the form of self-trapped holes

Received: September 14, 2023
Revised: October 2, 2023
Published: October 16, 2023

https://doi.org/10.1021/acs.jpcc.3c06180
J. Phys. Chem. C 2023, 127, 20965−20970

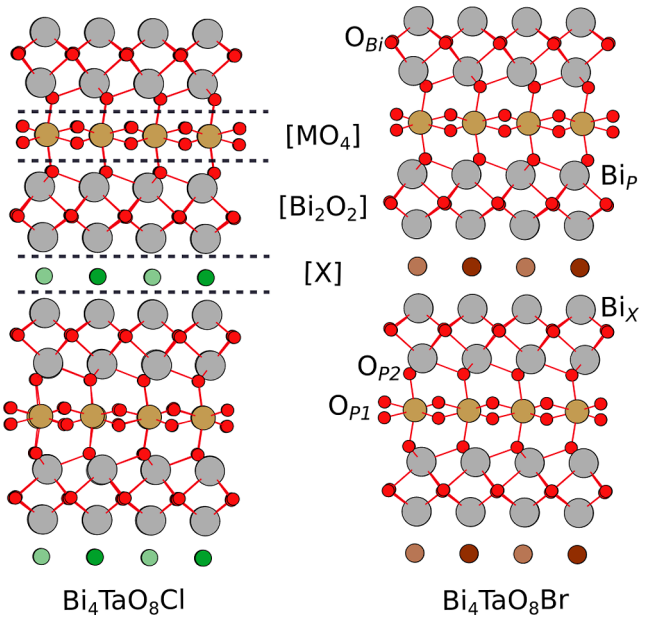

Figure 1. Crystal structure of Bi_4TaO_8X systems with the $P2_1cn$ space group. The elements Bi, Br, Cl, O, and Ta are shown with gray, brown, green, red, and yellow, respectively.

(V_K-centers), while in BiOCl they are centered around a single Bi atom.[11] In perovskite tantalates, holes have been found to localize mainly on a single oxygen site.[10] In contrast, we found that electron polarons are unstable in bismuth oxyhalides BiOX. However, in tantalates we observed that excess electrons can localize within a plane, displaying a two-dimensional gas-like nature. Since perovskite oxyhalides Bi_4TaO_8X are composed of three main blocks: perovskite ($[MO_4]$), halide ([X]), and bismuth−oxygen ($[Bi_2O_2]$), it is of great interest to explore the stability of all of the aforementioned polaronic states and compare with their counterparts in tantalates and oxyhalides.

In the present study, we aim to explore the polaronic configurations in perovskite oxyhalides Bi_4TaO_8X by using the hybrid functional *Perdew−Burke-Ernzerhof* [PBE0(α)].[12] We first find that the electron polarons are unstable in Bi_4TaO_8X similarly to our previous findings in BiOX materials. At variance, we observe that the structural heterogeneity in these materials leads to the formation of various hole polaronic states. In addition, we conduct an analysis of the energetics and structural distortions that are associated with the hole polarons. Our findings indicate that excess holes are highly localized at the perovskite block $[MO_4]$, displaying properties analogous to those in $NaTaO_3$. Finally, we show that bipolaronic trapping may arise due to the formation of O−O dimers when two holes are present in the system.

METHODS

To investigate hole polarons in Bi_4TaO_8X perovskite oxyhalides, we use the hybrid functional PBE0(α)[12] with D3 van der Waals interactions by Grimme[13] as implemented in the CP2K package.[14] In the PBE0 (α) calculations, we set the mixing parameter α at 0.26 for both Bi_4TaO_8Cl and Bi_4TaO_8Br. This value is obtained by employing the generalized Koopmans' theorem, which states that the single-particle level should not depend on its occupation. The level for which the condition is verified can be induced for example by a defect, such as an anion vacancy.[10,15] In particular, we choose here the oxygen vacancy, which exhibits a vertical (+1/0) transition within the band gap of both compounds considered here. With two different α values (0.25 and 0.5), we determine the unoccupied defect level in the neutral charge state and the occupied one in the +1 state. We use the method by Falletta et al.[16] to correct the finite-size errors related to the calculation of single-particle energy levels in charged supercells. We compute the high-frequency dielectric constants needed in the correction procedure at PBE level, and we find ϵ_∞ of 5.33 and 5.36 for Bi_4TaO_8Cl (BTOCl) and Bi_4TaO_8Br (BTOBr), respectively. The α-dependence of the single-particle levels for both materials is given in Figure 2.

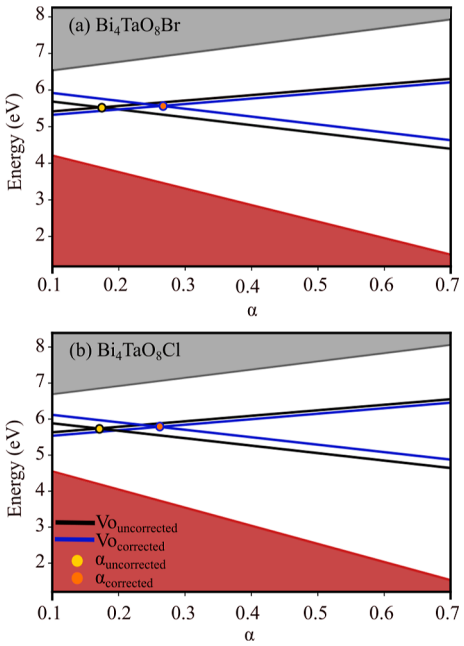

Figure 2. Band edges and single-particle levels of an oxygen vacancy (V_O) with respect to the fraction of Fock exchange α in Bi_4TaO_8Br (a) and Bi_4TaO_8Cl (b). The blue lines and orange circles represent the corrected levels and the corresponding corrected α. The black lines and yellow circles are uncorrected levels and the uncorrected α.

In all calculations, we use molecularly optimized (MOLOPT) basis sets[17] of the Gaussian type with a cutoff energy of 650 Ry to expand the electron density into plane waves. To characterize the core−valence interactions, we use Goedecker−Teter−Hutter pseudopotentials.[18] The auxiliary density matrix method[19] is used to increase the performance of Hartree−Fock exchange calculations. We consider a supercell ($2 \times 2 \times 1$) of perovskite oxyhalides Bi_4TaO_8X (X = Cl, Br) containing 224 atoms, with the orthorhombic space group $P2_1cn$ and the experimental lattice parameter as summarized in Table 1.

Table 1. Experimental Lattice Parameters and Band Gaps of the Considered Oxyhalides (from refs 20 and 21)

material	a (Å)	b (Å)	c (Å)	E_{gap}^{exp} (eV)
Bi_4TaO_8Cl	5.45	5.50	28.69	2.50
Bi_4TaO_8Br	5.47	5.51	29.22	2.55

https://doi.org/10.1021/acs.jpcc.3c06180
J. Phys. Chem. C 2023, 127, 20965−20970

RESULTS AND DISCUSSION

Electron and Hole Polarons. In Bi_4TaO_8X, the (001) surfaces are the most exposed facets.[22,23] Consequently, the photocatalytic activity of these materials will depend on the behavior of charges migrating in the *c* direction through the blocks consisting of a perovskite $[MO_4]$ block that is sandwiched between two fluorite $[Bi_2O_2]$ blocks and a single halogen [X] layer. Therefore, we assess the stability of the hole and electron polarons at each of these blocks. We begin by investigating the electron polaron stability. Due to the dominance of the Bi 6p and Ta 4d states in their conduction band, we add one electron to the system with varying initial structural distortions around the Ta site at the $[MO_4]$ block (we elongate one or several Ta−O bonds) and the Bi site at the $[Bi_2O_2]$ block (we elongate one or several Bi−O/X bonds). During the geometry optimization of all investigated structures, the electron delocalizes suggesting that the electron polarons are unstable in Bi_4TaO_8X.

In the case of hole polarons, we start by examining the possibility of halogen-related charge localization. We incorporate various structural distortions within the halogen [X] layer. This includes either elongating the Bi−X bonds (for single site localization) or shortening the X−X bonds in order to form X_2 dimers, also called V_k centers.[24] After optimizing the geometry, we find that the hole always ends up being delocalized, and the spin density is spread out throughout all of the O and X sites in whole Bi_4TaO_8X. This implies that, despite the fact that X−X distances in Bi_4TaO_8X are comparable with the intralayer ones in BiOX, the V_k centers are unstable in perovskite oxyhalides, in contrast to what we observed previously in BiOCl and BiOBr.[11] This difference in the behavior of holes can be explained by the fact that the VBM of Bi_4TaO_8X primarily consists of O 2p instead of Cl 3p or Br 4p like in the case in BiOX. Consequently, we explore the two blocks $[MO_4]$ and $[Bi_2O_2]$ that contain oxygen atoms to allow for polaronic configurations involving oxygen.

First, we investigate the hole polarons in the perovskite block by introducing a seed for polaron deformation by elongating two Ta−O bonds around an oxygen site. In Figure 3, we show the spin density of the hole after a full relaxation, where we see clearly that the hole polaron localizes mainly at one oxygen site and the four nearest oxygen neighbors within the (001) plane for BTOCl and BTOBr. This localization induces a structural distortion, where the Ta−O bonds are elongated due to an outward displacement of Ta atoms. The length of two Ta−O bonds increased by +0.2 and +0.1 Å (see Figure 3b,d) compared to the ones in the pristine structure of BTOCl (1.88 and 2.08 Å) and BTOBr (1.88 and 2.10 Å), respectively. Interestingly, the structural fingerprint (the elongation of two Ta−O bonds) of the hole polaron configuration in the perovskite block $[MO_4]$ of Bi_4TaO_8X is identical to the one in the orthorhombic $NaTaO_3$.[10] To promote hole localization at the apical oxygen (O_{P2}) connecting the two blocks $[MO_4]$ and $[Bi_2O_2]$, we elongated two Bi−O_{P2} bonds and the Ta−O_{P2} bond around this site. As seen in Figure 4a,b, the hole is localized mainly at the O_{P2} site and at two equatorial oxygens (O_{P1}) in BTOCl and BTOBr. In the corresponding structural deformation of the hole polaron, the length of two Bi−O_{P2} in BTOCl increases by 0.26 and 0.13 Å, and in the case of BTOBr these bonds become longer by 0.24 and 0.12 Å. The bond length of Ta−O_{P2} increases by 0.12 Å in both materials BTOCl and BTOBr.

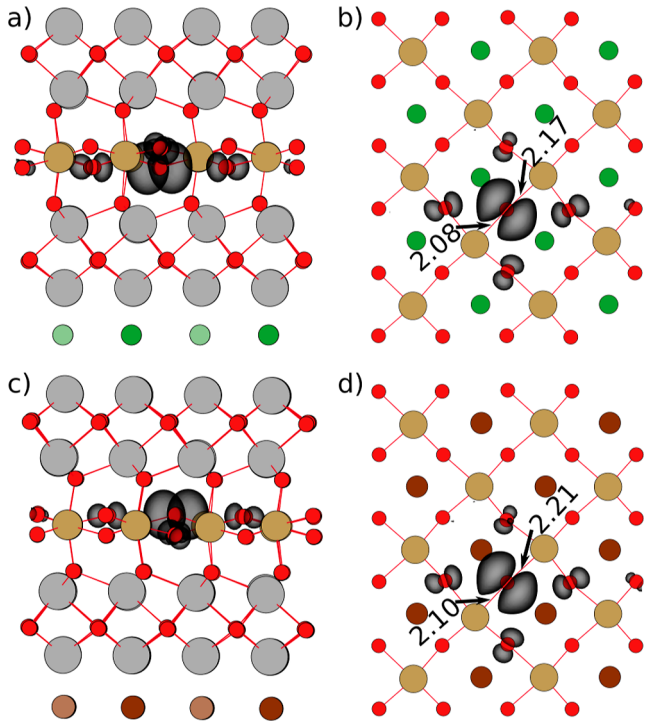

Figure 3. Spin density isosurface (0.045 e/Å^3) representations of (a) top and (b) side views of a self-trapped hole at the O_{P1} site in Bi_4TaO_8Cl and (c) top and (d) side views in Bi_4TaO_8Br.

To identify the hole localization mode at the oxygen site (O_{Bi}) in $[Bi_2O_2]$ blocks, we apply multiple structural distortions by elongating the Bi−O_{Bi} bonds in BTOCl and BTOBr. The geometrical optimizations lead to a state where the hole is localized, with spin density distributed mainly on the oxygen O_{Bi} and two nearest oxygens indicating that this type of localization is stable (see Figure 4c,d). We analyze the geometry of this polaronic configuration, and we find that the distortion is related to an increase of four Bi−O_{Bi} bonds, two of them by 0.2 Å and the others by 0.1 Å compared to the pristine structure of both materials. It is worth noting that the hole localization centered on a single oxygen localization found here was not found to be stable in BiOCl and BiOBr, despite the similarities in the structural features of $[Bi_2O_2]$ block in both material families.[11] The last localization mode worth exploring is around a single Bi site, similar to the ones previously reported in $BiVO_4$ and oxyhalides (BiOCl and BiOBr).[11,25,26] In this polaron configuration in $BiVO_4$, the lengths of some Bi−O bonds increase and others decrease.[25,26] In the case of oxyhalides (BiOBr and BiOCl), the hole polaron at the Bi site causes a symmetrical contraction of both Bi−O bonds and Bi−X bonds.[11] Considering that there are two distinct Bi sites in the perovskite oxyhalide structure, the Bi_P site at the interface with $[MO_4]$ block and the Bi_X site within $[Bi_2O_2]$ block (see Figure 1), we apply structural distortions around both of them. We first investigate the Bi_X site by shortening the Bi−O/X bonds and introducing a hole into the system. After the geometry optimization, we find that the hole is delocalized with the spin density distributed over all the O and X sites in both BiTOX materials. However, in the case of the Bi_P site, after geometry relaxation initiated with shortened Bi−O bonds, we find the hole to be localized with the spin density centered around the Bi_P site. The hole density can also be found at eight neighboring oxygen sites, four belonging to

https://doi.org/10.1021/acs.jpcc.3c06180
J. Phys. Chem. C 2023, 127, 20965−20970

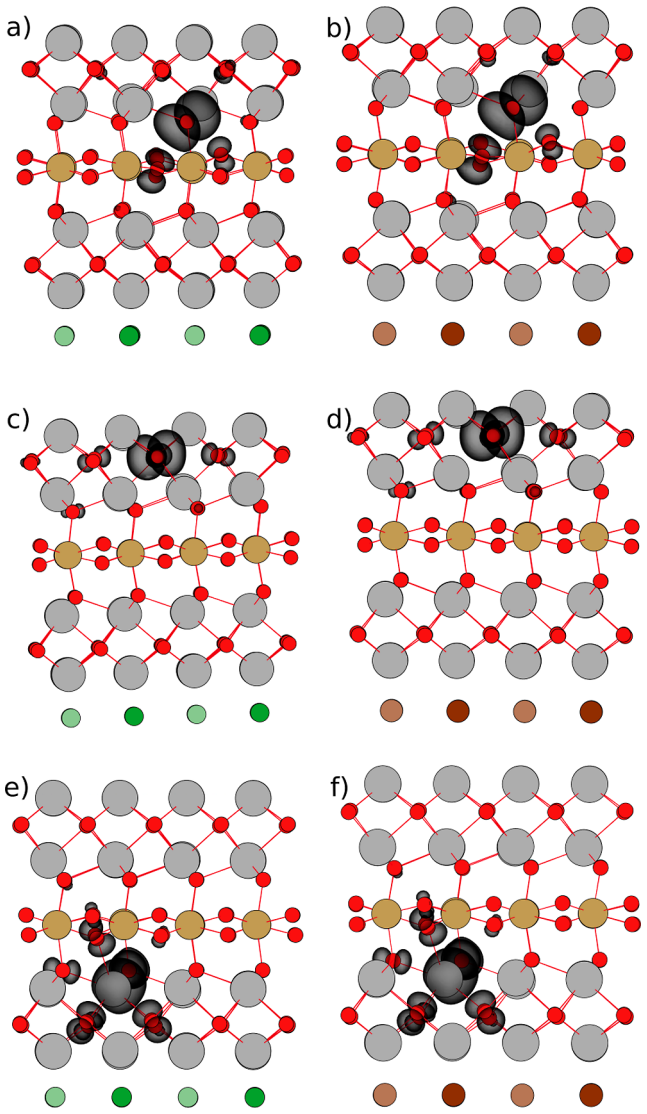

Figure 4. Spin density isosurface (0.045 e/Å^3) representations: (a), (c), and (e) of a self-trapped hole in Bi_4TaO_8Cl at O_{Bi}, O_{P2}, and Bi site, respectively. (b), (d), and (f) of a self-trapped hole in Bi_4TaO_8Br at O_{Bi}, O_{P2}, and Bi site, respectively.

the $[Bi_2O_2]$ block and four to the $[MO_4]$ block as illustrated in Figure 4e,f. In this polaron configuration, the length of three Bi−O bonds at the $[Bi_2O_2]$ block becomes shorter by 0.12 Å, and the length of the Bi−O bonds with two perovskite apical oxygens becomes longer by 0.06 Å in BTOCl and BTOBr. Furthermore, we observe a strong upward displacement of the perovskite equatorial oxygen, resulting in the shortening of the distance between Bi and O_{P1} by 0.22 Å in BTOBr and 0.3 Å in BTOCl.

To assess the stability of the different polaronic states, we characterize them by calculating binding energies, defined as follows

$$E_b = E_{+1}[\text{polaron}] - E_0\,[\text{pristine}] + \epsilon_v + E_{corr}$$

where E_0 is the energy of the neutral nondistorted structure, E_q is the energy of the fully relaxed polaron state, ϵ_v is the position of the VBM, and E_{corr} is the electrostatic finite-size correction, calculated according to the scheme proposed by Freysoldt, Neugebauer, and Van de Walle (FNV).[27]

Table 2 presents the calculated binding energies of hole polarons in the various configurations that we identified. The

Table 2. Calculated Binding Energies of Hole Polarons in Different Configurations[a]

	E_b(hole) (eV)				
	O_{P1}	O_{P2}	O_{Bi}	Bi	O−O
Bi_4TaO_8Cl	−0.67	−0.55	−0.36	−0.51	−0.94
Bi_4TaO_8Br	−0.70	−0.59	−0.38	−0.54	−0.96

[a]In the case of the O−O bipolaron, we report the binding energy per one hole.

obtained binding energies are all negative for both materials, meaning that self-trapped holes are stable in both BTOCl and BTOBr. Furthermore, we find that the binding energies of the polaron at the oxygen sites of $[MO_4]$ are lower than the ones of $[Bi_2O_2]$, suggesting that the hole localization at the site O_{P1} is the most stable. In BTOBr the stability is slightly stronger than in BTOCl, which is in agreement with the small difference in the amplitude of the structural distortion observed in both materials. We remark that the binding energies of the hole polarons are comparable to the ones reported for $NaTaO_3$,[10] suggesting similar behavior of excess holes in these materials. At the Bi site the binding energies of the polarons are less negative than the ones at the O_P site and lower than in the O_{Bi} configuration, meaning that it is the most stable localization mode within the $[Bi_2O_2]$ block. On the other hand, the binding energies related to the hole localization at the Bi site are equal in BTOCl and BTOBr. We also note that this polaronic configuration is significantly more stable than the ones found in BiOBr and BiOCl despite the likeness of the structure of the $[Bi_2O_2]$ block.[11] Moreover, we find that the stability of the hole localization is less affected by the halide size in contrast with our previous findings in BiOX oxyhalide.[11]

Hole Bipolaron. In addition to single-hole polarons, we investigate what happens when two holes are localized in the same region. It has been reported that in $SrTiO_3$ and $BiVO_4$ two holes can form O_2^{2-} peroxides (bipolarons) due to O−O dimerization.[28−30] Therefore, we consider charge localization on various oxygen pairs in both the $[MO_4]$ and $[Bi_2O_2]$ blocks of BTOCl and BTOBr. The spacing between two chosen oxygen atoms is decreased to 1.4 Å to form dimer structures. Then, two holes are added to the system in a low-spin state. After relaxation, we observe various bipolaronic configurations in both blocks characterized by the O−O bond length of about 1.47 Å. Figure 5, illustrates the structure of the most stable bipolaron in BTOCl and BTOBr, where the dimer is formed by an apical and an equatorial oxygen O_{P1}−O_{P2}. We also show the difference between the charge density of a charged system including a dimer and a neutral system in which the two oxygen atoms are in their pristine positions. To assess the stability of this bipolaronic configuration, we calculate the binding energy with respect to the pristine state

$$E_b = E_{+2}[\text{polaron}] - E_0\,[\text{pristine}] + 2\epsilon_v + E_{corr}$$

where, E_{+2} is the energy of the fully relaxed polaron state and the other quantities are defined in the previous section. We find that the binding energy of the hole bipolaron (as referred to the delocalized state) is about −1.89 and −2.02 eV for BTOCl and BTOBr, respectively. This corresponds to −0.94 and −1.01 eV per hole, which is significantly lower than the most stable single hole polaron at the O_{P1} site.

https://doi.org/10.1021/acs.jpcc.3c06180
J. Phys. Chem. C 2023, 127, 20965−20970

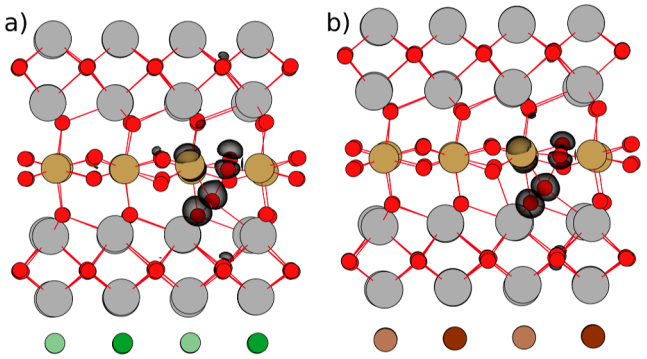

Figure 5. Charge density differences between systems with and without the dimer bipolaronic configuration in (a) Bi_4TaO_8Cl and (b) Bi_4TaO_8Br.

Overall, we found that excess holes are strongly localized in perovskite oxyhalides BiTOX. They exhibit significant binding energies both in states related to single and double-hole localization. The charge localization could have both detrimental and beneficial effects on the photocatalytic properties of these materials. Charge trapping is known to reduce mobilities and introduce deep levels and additional recombination channels.[31,32] On the other hand, other studies showed that charge localization can have beneficial effects on carrier lifetimes (by reducing the overlap between opposite charges)[30] and photocatalytic reactions (by e.g., improving the energy alignment of charges with redox potentials).[33,34] While we suggest that the high stability of hole polarons can have an important effect on the behavior of photogenerated charges in perovskite bismuth oxyhalides, further studies are needed to fully understand their influence on the photocatalytic properties.

CONCLUSIONS

In this study, we investigated the behavior of photogenerated holes and electrons in bismuth perovskite oxyhalides Bi_4TaO_8X. We first demonstrated that the formation of an electron polaron in Bi_4TaO_8X oxyhalides is unfavorable, similar to the case of BiOX oxyhalides and the $NaTaO_3$ perovskite. However, it is predicted that hole polaron localization is stable and shows diverse configurations depending on the local environment. Our analysis suggests that the most favorable single-polaronic state is the one where the hole is self-trapped on one equatorial oxygen at the perovskite block with a small fraction of density spread over four neighboring oxygen atoms. This localization caused structural distortions in which two Ta−O bonds are elongated by about 0.2 and 0.1 Å in BTOBr and BTOCl. In contrast with BiOBr and BiOCl oxyhalides, halogen size has a negligible impact on the hole polaron configuration stability and structural distortion in BTOBr and BTOCl. We also show that in the presence of two holes this material tends to localize them by forming O_2^{2-} peroxide due to O−O dimerization. Finally, we believe that these insights into the behavior of photogenerated carriers in the Bi_4TaO_8X series might serve as a reference for additional investigation.

AUTHOR INFORMATION

Corresponding Author

Julia Wiktor − *Department of Physics, Chalmers University of Technology, SE-412 96 Gothenburg, Sweden;* orcid.org/0000-0003-3395-1104; Email: julia.wiktor@chalmers.se

Author

Hassan Ouhbi − *Department of Physics, Chalmers University of Technology, SE-412 96 Gothenburg, Sweden;* orcid.org/0000-0001-7371-4782

Complete contact information is available at: https://pubs.acs.org/10.1021/acs.jpcc.3c06180

Notes

The authors declare no competing financial interest.

ACKNOWLEDGMENTS

The authors acknowledge funding from the "Area of Advance Materials Science" at Chalmers University of Technology and the Swedish Research Council (2019-03993). The computations were performed on resources provided by the Swedish National Infrastructure for Computing (SNIC) at NSC, C3SE, and PDC. This work was supported by the Chalmers Gender Initiative for Excellence (Genie).

REFERENCES

(1) Bouri, M.; Ninova, S.; Ouhbi, H.; Vonrüti, N.; Aschauer, U. Surface Chemistry of Perovskite Oxynitride Photocatalysts: A Computational Perspective. *Chimia* **2021**, *75*, 202.

(2) Ouhbi, H.; Aschauer, U. Nitrogen Loss and Oxygen Evolution Reaction Activity of Perovskite Oxynitrides. *ACS Mater. Lett.* **2019**, *1*, 52−57.

(3) Ueda, K.; Minegishi, T.; Clune, J.; Nakabayashi, M.; Hisatomi, T.; Nishiyama, H.; Katayama, M.; Shibata, N.; Kubota, J.; Yamada, T.; et al. Photoelectrochemical Oxidation of Water Using $BaTaO_2N$ Photoanodes Prepared by Particle Transfer Method. *J. Am. Chem. Soc.* **2015**, *137*, 2227−2230. PMID: 25650748

(4) Kunioku, H.; Higashi, M.; Tomita, O.; Yabuuchi, M.; Kato, D.; Fujito, H.; Kageyama, H.; Abe, R. Strong hybridization between Bi-6s and O-2p orbitals in Sillén−Aurivillius perovskite Bi_4MO_8X (M = Nb, Ta; X = Cl, Br), visible light photocatalysts enabling stable water oxidation. *J. Mater. Chem. A* **2018**, *6*, 3100−3107.

(5) Kato, D.; Hongo, K.; Maezono, R.; Higashi, M.; Kunioku, H.; Yabuuchi, M.; Suzuki, H.; Okajima, H.; Zhong, C.; Nakano, K.; et al. Valence Band Engineering of Layered Bismuth Oxyhalides toward Stable Visible-Light Water Splitting: Madelung Site Potential Analysis. *J. Am. Chem. Soc.* **2017**, *139*, 18725−18731. PMID: 29210576

(6) Ogawa, K.; Suzuki, H.; Walsh, A.; Abe, R. Orbital Engineering in Sillén−Aurivillius Phase Bismuth Oxyiodide Photocatalysts through Interlayer Interactions. *Chem. Mater.* **2023**, *35*, 5532−5540.

(7) Kusainova, A. M.; Zhou, W.; Irvine, J. T.; Lightfoot, P. Layered Intergrowth Phases Bi_4MO_8X (X = Cl, M = Ta and X = Br, M = Ta or Nb): Structural and Electrophysical Characterization. *J. Solid State Chem.* **2002**, *166*, 148−157.

(8) Wei, S.; Xu, X. Boosting photocatalytic water oxidation reactions over strontium tantalum oxynitride by structural laminations. *Appl. Catal., B* **2018**, *228*, 10−18.

(9) Fujito, H.; Kunioku, H.; Kato, D.; Suzuki, H.; Higashi, M.; Kageyama, H.; Abe, R. Layered perovskite oxychloride Bi_4NbO_8Cl: a stable visible light responsive photocatalyst for water splitting. *J. Am. Chem. Soc.* **2016**, *138*, 2082−2085.

(10) Ouhbi, H.; Wiktor, J. Polaron formation and hopping in tantalate perovskite oxides: $NaTaO_3$ and $KTaO_3$. *Phys. Rev. B* **2021**, *104*, 235158.

(11) Ouhbi, H.; Wiktor, J. Ab Initio Insights into Charge Localization in Bismuth Oxyhalides BiOX (X = F, Cl, Br, I). *J. Phys. Chem. C* **2022**, *126*, 19956−19961.

(12) Perdew, J. P.; Ernzerhof, M.; Burke, K. Rationale for mixing exact exchange with density functional approximations. *J. Chem. Phys.* **1996**, *105*, 9982−9985.

(13) Grimme, S.; Ehrlich, S.; Goerigk, L. Effect of the damping function in dispersion corrected density functional theory. *J. Comput. Chem.* **2011**, *32*, 1456−1465.

(14) VandeVondele, J.; Krack, M.; Mohamed, F.; Parrinello, M.; Chassaing, T.; Hutter, J. Quickstep: Fast and accurate density functional calculations using a mixed Gaussian and plane waves approach. *Comput. Phys. Commun.* **2005**, *167*, 103−128.
(15) Bischoff, T.; Wiktor, J.; Chen, W.; Pasquarello, A. Nonempirical hybrid functionals for band gaps of inorganic metal-halide perovskites. *Phys. Rev. Mater.* **2019**, *3*, 123802.
(16) Falletta, S.; Wiktor, J.; Pasquarello, A. Finite-size corrections of defect energy levels involving ionic polarization. *Phys. Rev. B* **2020**, *102*, 041115.
(17) VandeVondele, J.; Hutter, J. Gaussian basis sets for accurate calculations on molecular systems in gas and condensed phases. *J. Chem. Phys.* **2007**, *127*, 114105.
(18) Goedecker, S.; Teter, M.; Hutter, J. Separable dual-space Gaussian pseudopotentials. *Phys. Rev. B: Condens. Matter Mater. Phys.* **1996**, *54*, 1703−1710.
(19) Guidon, M.; Hutter, J.; VandeVondele, J. Auxiliary Density Matrix Methods for Hartree−Fock Exchange Calculations. *J. Chem. Theory Comput.* **2010**, *6*, 2348−2364.
(20) Kan, Y.; Teng, F.; Yang, Y.; Xu, J.; Yang, L. Direct conversion mechanism from BiOCl nanosheets to BiOF, $Bi_7F_11O_5$ and BiF_3 in the presence of a fluorine resource. *RSC Adv.* **2016**, *6*, 63347−63357.
(21) An, H.; Du, Y.; Wang, T.; Wang, C.; Hao, W.; Zhang, J. Photocatalytic properties of BiOX (X = Cl, Br, and I). *Rare Met.* **2008**, *27*, 243−250.
(22) Li, L.; Han, Q.; Tang, L.; Zhang, Y.; Li, P.; Zhou, Y.; Zou, Z. Flux synthesis of regular Bi_4TaO_8Cl square nanoplates exhibiting dominant exposure surfaces of 001 crystal facets for photocatalytic reduction of CO_2 to methane. *Nanoscale* **2018**, *10*, 1905−1911.
(23) Jia, J.; Liang, Y.; Yang, G.; Yang, J.; Zhang, X.; Xiong, Z.; Sa, K.; Zeng, Z.; Han, Y. Molten-salt-mediated synthesis of Na+ doped Bi_4TaO_8Cl nanosheets with exposed 001 facets for enhanced photocatalytic degradation. *J. Alloys Compd.* **2023**, *932*, 167461.
(24) Känzig, W. Electron Spin Resonance of V_1-Centers. *Phys. Rev.* **1955**, *99*, 1890−1891.
(25) Wiktor, J.; Ambrosio, F.; Pasquarello, A. Role of Polarons in Water Splitting: The Case of $BiVO_4$. *ACS Energy Lett.* **2018**, *3*, 1693−1697.
(26) Liu, T.; Cui, M.; Dupuis, M. Hole Polaron Transport in Bismuth Vanadate $BiVO_4$ from Hybrid Density Functional Theory. *J. Phys. Chem. C* **2020**, *124*, 23038−23044.
(27) Freysoldt, C.; Neugebauer, J.; Van de Walle, C. G. Fully ab initio finite-size corrections for charged-defect supercell calculations. *Phys. Rev. Lett.* **2009**, *102*, 016402.
(28) Chen, H.; Umezawa, N. Hole localization, migration, and the formation of peroxide anion in perovskite $SrTiO_3$. *Phys. Rev. B: Condens. Matter Mater. Phys.* **2014**, *90*, 035202.
(29) Strand, J.; Dicks, O. A.; Kaviani, M.; Shluger, A. L. Hole trapping in amorphous HfO_2 and Al_2O_3 as a source of positive charging. *Microelectron. Eng.* **2017**, *178*, 235−239.
(30) Ambrosio, F.; Wiktor, J.; De Angelis, F.; Pasquarello, A. Origin of Low Electron−Hole Recombination Rate in Metal Halide Perovskites. *Energy Environ. Sci.* **2018**, *11*, 101−105.
(31) Guo, C.; Meng, X.; Fu, H.; Wang, Q.; Wang, H.; Tian, Y.; Peng, J.; Ma, R.; Weng, Y.; Meng, S.; et al. Probing nonequilibrium dynamics of photoexcited polarons on a metal-oxide surface with atomic precision. *Phys. Rev. Lett.* **2020**, *124*, 206801.
(32) Cheng, C.; Fang, Q.; Fernandez-Alberti, S.; Long, R. Controlling charge carrier trapping and recombination in $BiVO_4$ with the oxygen vacancy oxidation state. *J. Phys. Chem. Lett.* **2021**, *12*, 3514−3521.
(33) Ambrosio, F.; Wiktor, J. Strong Hole Trapping Due to Oxygen Dimers in BiVO4: Effect on the Water Oxidation Reaction. *J. Phys. Chem. Lett.* **2019**, *10*, 7113−7118. PMID: 31657932
(34) Ricciarelli, D.; Kaiser, W.; Mosconi, E.; Wiktor, J.; Ashraf, M. W.; Malavasi, L.; Ambrosio, F.; De Angelis, F. Reaction Mechanism of Photocatalytic Hydrogen Production at Water/Tin Halide Perovskite Interfaces. *ACS Energy Lett.* **2022**, *7*, 1308−1315.

https://doi.org/10.1021/acs.jpcc.3c06180
J. Phys. Chem. C 2023, 127, 20965−20970